Photoluminescence Excitation in Nanocomposites Polyvinylpyrrolidone/ZnO

V.I. Fediv[1], G.Yu. Rudko[2,3], O.F. Isaieva[2], E.G. Gule[2], O.I. Olar[1]

[1] *Department of Biological Physics and Medical Informatics, Bukovinian State Medical University,
42, Kobylyanska Str., 58000 Chernivtsi, Ukraine*
[2] *V. Lashkaryov Institute of Semiconductor Physics of National Academy of Sciences of Ukraine,
45, Pr. Nauky, 03028 Kiev, Ukraine*
[3] *National University "Kyiv-Mohyla Academy", 2, Skovorody Str., 04070 Kiev, Ukraine*

ZnO nanoparticles embedded in polyvinylpyrrolidone matrix were fabricated in situ by colloidal method with environmentally friendly reaction conditions. The colloid was used to form solid nanocomposite polyvinylpyrrolidone/ZnO, and optical properties of the material were studied. Two types of emission were identified in the nanocomposite: one originates from the polymeric matrix another is related the defect states in ZnO nanoparticles. Specific way of light emission excitation via energy transfer from the polymeric matrix to nanoparticles was observed.

Keywords: Nanocomposite, Photoluminescence, Energy transfer, ZnO.

1. INTRODUCTION

Recently, many researchers have focused on the fabrication and luminescent properties of nano-phosphors. In particular, inorganic-organic hybrid nanocomposites are an example of the materials, which became promising as a creative alternative to the industrially used phosphors. Development of new phosphors and investigation of luminescence mechanisms are the main aspects of current research. Among the components for nanocomposites fabrication the recognized favourites are semiconductor nanoparticles (NPs) that are used as a base of composites and fillers, respectively. By variation of different components, changing of NP sizes and tuning of interfacial conditions, wide assortment of nanocomposites with highly adjustable properties can be produced.

ZnO nanoparticles are widely employed in the fundamental research and commercial applications (field emitters, ultraviolet lasers and diodes, piezoelectric devices, fluorescence labels in medicine and biology) [1, 2]. The controlled synthesis of ZnO NPs and in-depth understanding of the physical properties are the key issues for the future development of ZnO-based devices. Different chemical methods of nanosized ZnO preparation have been reported, like sol-gel method [3], precipitation in alcoholic medium [4], polyolsynthesis [5], etc. General trend in chemical methods is application of various capping agents such as polyvinylpirrolidone (PVP), thiols, etc., that are used to arrest the growth of particles with time [6, 7]. Different preparation techniques lead to large diversity of structures and surface properties of ZnO particles which causes wide assortment of luminescent characteristics of these nanomaterials. Emission of ZnO particles depends on the method of fabrication [8, 9], annealing conditions in various environments [10, 11], presence of dopants [12] and coatings [13-15]. Generally, ZnO exhibits two kinds of emissions: one is an ultraviolet near band-edge emission at approximately 380 nm and the other is a visible deep level emission in the range from 450 to 730 nm.

Among possible capping agents PVP is a great stabilizer which prevents the aggregation of NPs via the repulsive forces that arise from its hydrophobic carbon chains that extend into solvents and interact with each other (steric hindrance effect). PVP is a remarkably stable non-toxic, non-ionic polymer with $C = O$, $C - N$ and CH_2 functional groups. It is widely used in NPs synthesis. An important feature of PVP is the existence of carbonyl oxygens which can form hydrogen bonds with solvent molecules. PVP is a polymer with inert physicochemical properties over a broad range of pH values.

Here, we report on the synthesis of ZnO NPs by the in-situ colloidal technique with environmentally friendly reaction conditions and consequent production of solid PVP/ZnO nanocomposites. The luminescent properties of the material are studied.

2. EXPERIMENTAL

In a typical synthesis (see Fig. 1) [Zn (Ac)$_2$ ·2H$_2$O] was dissolved completely in water by vigorous stirring at about 50 °C. The solution was chilled to 0 °C in an ice bath. Tetramethylammonium hydroxide (TMAH) was slowly added drop-wise using a dropping funnel to the above cooled solution under stirring. Finally, the reaction vessel was heated to 80 °C for 2 hrs. During this time the precipitation of NPs occured. The product obtained was added to the water solution of PVP, and, as a result, colloidal solutions of ZnO NPs in PVP were obtained. For characterization of NPs sizes we measured the absorption edge of the solution (see insert in Fig 2, b). As the absorption edge of PVP lies at about 5 eV [16], the observed absorption edge in near UV is ascribed to the band-to band transitions in NPs. The spectral position of NP's absorption edge is closed to with the one in bulk ZnO, i.e., the sizes of colloidal ZnO NPs are sufficiently large for quantum confinement effects to be not observed.
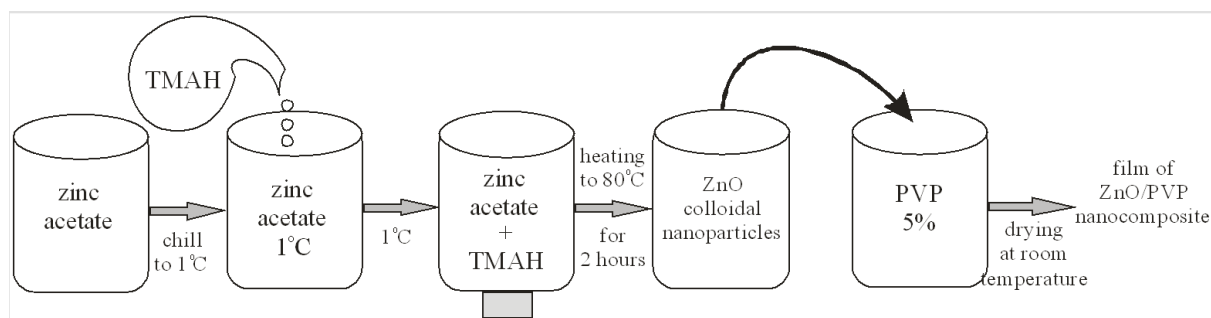
Fig. 1 – Synthezes steps of PVP/ZnO nanocomposite

To obtain thin solid films of composites the colloidal solutions of ZnO NPs were placed in glass Petri dishes and then dried at room temperature in a closed vessel containing an absorbent. The same amount of pure PVP was also dried in a Petri dish to obtain a reference sample of solid PVP film.

Optical absorption spectra were taken on a UV/VIS Spectrometer (Agilent Cary 60). For photoluminescence studies, the emission and excitation spectra were recorded on a Fluorescence Spectrophotometer (SHIMADZU RF-1501). All measurements were done at ambient conditions.

3. RESULTS

Fig. 2a-c shows photoluminescence (PL) and photoluminescence excitation (PLE) spectra of pure PVP (a) and PVP/ZnO nanocomposite (b,c). The UV-VIS absorption spectrum of PVP/ZnO nanocomposite is shown in the inset to Fig. 2b and demonstrates strong absorption of nanocomposite below 380 nm.

It is seen that room temperature PL bands of both nanocomposite and pure PVP are rather wide. PVP is
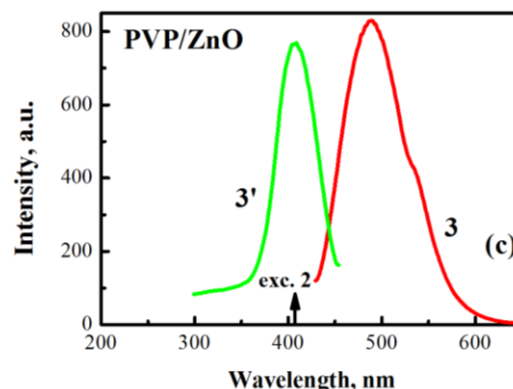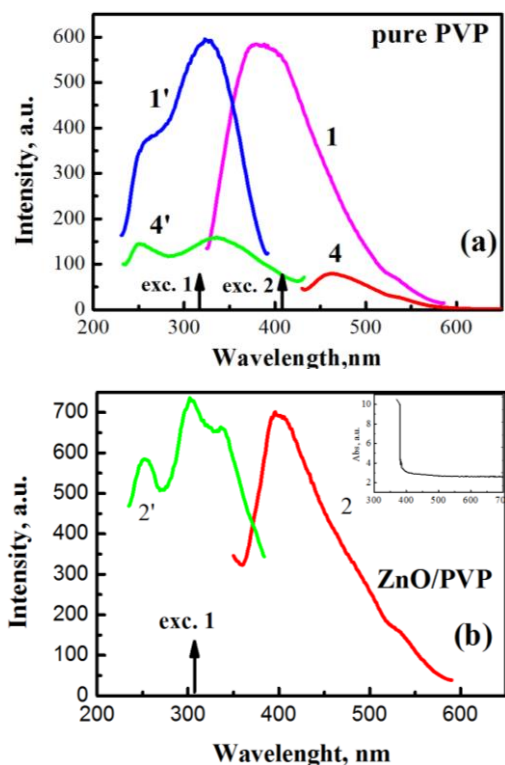

Fig. 2 – Excitation and emission spectra of pure PVP (a) and PVP/ZnO (b, c) nanocomposites measured at room temperature. PL spectra were measured at the excitation: $1,2 - \lambda_{exc1} = 308$ nm (shown by the arrow exc.1), $3,4 - \lambda_{exc2} = 408$ nm (shown by the arrow exc. 2). PLE spectra were detected at: $1', 2' - 408$ nm, $3',4' - 480$ nm. Inset: UV-VIS absorption spectrum of PVP/ZnO nanocomposite

emissive in the near UV and violet-blue ranges. The maximum of PL spectrum 1 of pure PVP (Fig. 2a), that is measured under excitation $\lambda_{exc1} = 308$ nm (4,03 eV), is observed at 390 nm (3,17 eV).

The PLE spectrum of the above PL band of PVP (390 nm) was detected close to the maximum of this band, namely, at 408 nm (3,03 eV). PLE spectrum of PVP is rather wide; presumably, it is comprised of at least two excitation peaks around 250 nm (~ 4.96 eV) and 325 nm (~ 3.81 eV) that strongly overlap. These excitation bands were attributed in [16, 17] to the electronic transitions in PVP molecular orbitals due to the presence of C = O and N-C groups, respectively.

PL spectrum of nanocomposite ZnO/PVP (Fig. 2b, spectrum 2) was measured under excitation in the near UV range ($\lambda_{exc1} = 308$ nm) and the maximum of PL was observed at ~ 408 nm. The corresponding PLE spectrum (Fig. 2b, spectrum 2′) was detected close to the maximum of the PL band 2 (namely, at 408 nm). It is seen that, at equivalent excitation conditions PL spectra of both materials are similar; the same holds true for PLE spectra. However, under different excitation conditions nanocomposite demonstrates one more emission band. This emission band can be excited by the light quanta with lower energies. Fig. 2c demontrates the PL spectrum of ZnO/PVP nanocomposite obtained at $\lambda_{exc2} = 408$ nm (curve 3, Fig. 2c). Maximum of the low energy emission band 3 occurs at ~ 480 nm. The corresponding PLE spectrum

(curve 3′, Fig. 2c). was measured at the detection at 480 nm. The maximum of PLE band 3′ occurs at ~ 408 nm. Note, that the spectral position of the PLE band 3′ is close to the maximum of the PL band 2.

4. DISCUSSION

The base of our composite – polymer PVP – demonstrates the known light-emitting features. The origin of the observed PL band 390 nm has been discussed in literature [18-20]. In [18, 19] similar emission band of PVP was ascribed to $\pi \leftarrow n\pi^*$ transition of PVP molecule. According to [20], the violet-blue emission band of PVP is attributed to the radiative relaxation of electrons from the lowest unoccupied molecular orbitals (LUMO) to the highest occupied molecular orbitals (HOMO) in PVP. As it was noticed above, the excitation of this PL band occurs via the energy levels emerging due to the presence of C = O and N-C groups [16, 17].

Comparing Fig. 2a and Fig. 2b, one can note that PL bands of both polymeric matrix and nanocomposite are similar at the excitation in the near UV range (λ_{exc1}); the PLE bands of both materials almost coinside as well. Therefore, it is natural to suggest that PL and PLE bands (curves 2 and 2′, respectively) observed in the nanocomposite samples have the same origin as the corresponding bands of polymer (curves 1 and 1′), i.e., that the spectra 2 and 2′ are related to the polymeric constituent of our nanocomposite. Note that in nanocomposite the emission band 2 is somewhat narrower than PL band 1 of pure PVP and is shifted to longer wavelengths. Provided PL band 2 is, indeed, emitted by the polymeric constituent of nanocomposite, the narrowing and shift can be caused by the presence of ZnO NPs: the NPs partly absorb the light emitted by the matrix. Due to the reabsorption of the polymer-emitted light by NPs, the short wavelength wing of the emission band 2 is diminished. In such a way, the absorption by NPs leads to the narrowing of the emission band and its apparent long wavelength shift.

Quite different PL and PLE spectra of ZnO/PVP (curves 3 and 3′, Fig. 2c, λ_{exc2}) can be interpreted as a signature of ZnO NPs that are present in the nanocomposite. This interpretation is corroborated by the fact that similar spectra are frequently observed in ZnO nanocrystals [21-28]. One more proof of the ZnO-related origin of PL band 3 can be obtained by comparing this emission with the PL spectrum of the unloaded polymer measured at the $\lambda_{exc2} = 408$ nm (see curve 4 in Fig. 2a). It is seen that the emission of pure PVP (curve 4) in the green spectral range is very weak and its shape does not resemble the band 3. Curve 4 can be interpreted as a residual emission of the peak 1 obtained under "inappropriate" (far from optimal) excitation conditions. Moreover, the PLE measurements (see 4′ in Fig. 2a) demonstrate that weak emission 4 is excited in the spectral range that coinsides with the excitation of PL band 1 and absolutely does not resemble the PLE band 3′. Therefore, one can conclude that radiative transitions which give rise to PL band 4 occur within the same manyfold of energy levels as the one giving rise to PL band 1 (Fig. 2a), i.e., they occur within the polymeric

matrix. Based on the above considerations, we interpret PL band 3 as the emission of ZnO NPs. The suggestions as to the origin of this emission can be found in literature. Green emission of ZnO NPs with ~ 480 nm wavelength (2.54 eV) can be related to the electron transition from the deep donor level of the ionized oxygen vacancies to the valence band [22]. In [23-28] it was suggested that green emission appears as the result of the transitions from the conduction band of ZnO nanocrystals to the anti-site oxygen Ozn level that is located at 2.38 eV below the conduction band. Keeping in mind that PL band 3 is rather wide, both these interpretations are applicable.

It should be stressed that PL spectrum 3 (Fig. 2c) was measured under the conditions when the excitation wavelength coinsides with the maximum of PL band 2 (Fig. 2b), namely, at 408 nm excitation. In other words, the spectral position of the excitation band of NPs emission coinsides with the spectral position of the emission band of polymer.

To illustrate the processes occurring in the unloaded polymer and PVP/ZnO nanocomposite we propose the scheme (Fig. 3) that is based on the above experimental data. Fig. 3a shows the known energy levels diagram of PVP polymer [29]. We use this diagram to analyze our experimental data on pure PVP (Fig. 2a). We also propose the diagram of ZnO/PVP nanocomposite and corresponding electronic transitions in it (Fig. 3b). The energies of all levels are counted from the vacuum level.

In accordance with the diagram in Fig. 3a wide PLE band of PVP (Fig. 2a, curve 2′) can be ascribed both to the transitions between HOMO and LUMO states of polymeric molecules and the transitions from HOMO states to shallow defect states of polymer. Here we illustrate the transitions occurring under the illumination with the light $\lambda_{exc1} = 308$ nm and $\lambda_{exc2} = 408$ nm (shown by the arrows exc.1 and exc.2, correspondingly). Emission of PVP is caused by the radiative transitions involving the levels from the manifold of defect states. This interpretation agrees both with our data and the data of [18-20]. Depending on the excitation wavelength the observed PL bands are wider (arrow 1) or narrower (arrow 4).

The diagram of the energy states of ZnO/PVP nanocomposite (Fig. 3b) includes two sets of energy levels corresponding to the composite constituents - the PVP states (the same as in Fig. 3a) and the states of ZnO NPs. Valence (VB) and conduction (CB) bands of ZnO are shown, as well as defect-related levels within the band gap of NP [22-28]. Despite a very wide variety of possible defects in ZnO we have restricted the diagram to only two defect levels that are relevant to our samples. The possible transitions with the absorption and emission of light are also shown.

Using this diagram one can analyze the transitions responsible for the spectra in Figs. 2a, b, c in detail.

The incident UV light (exc.1) causes the transition from HOMO to LUMO states of polymeric matrix in nanocomposite. After relaxation the photoexcited carriers recombine and produce the PL band 2 (see curve 2 in Fig. 2b and arrow (2) in Fig. 3b). All these processes occur within the polymeric constituent of nanocomposite.
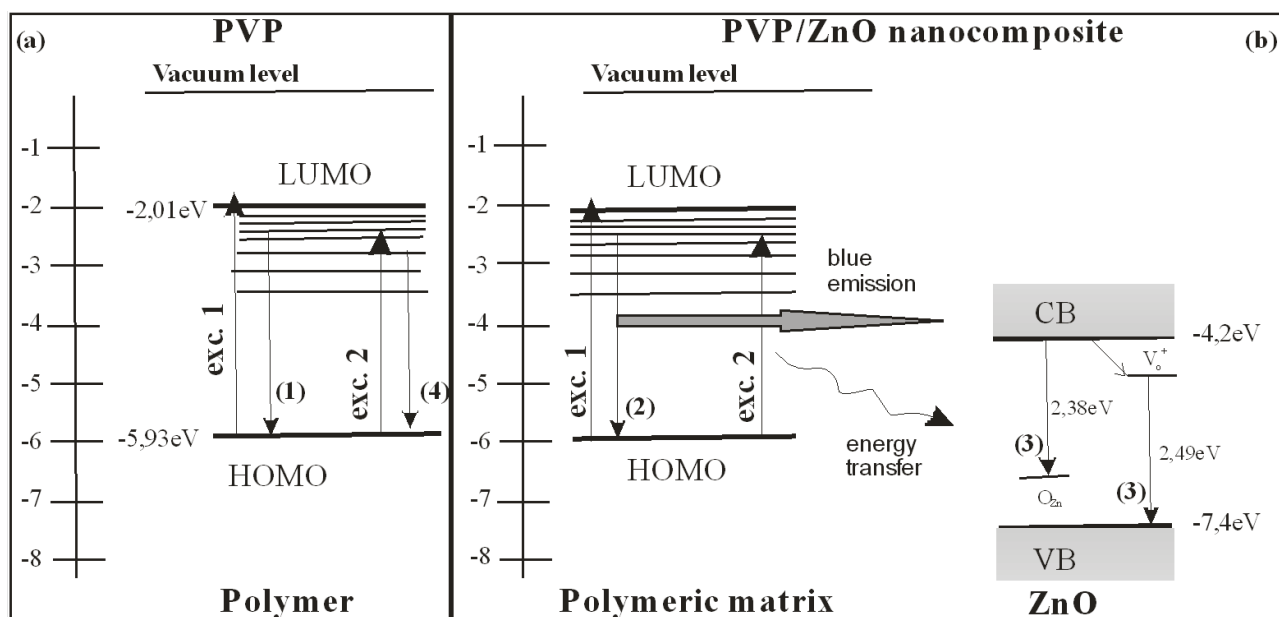
Fig. 3 – Schematic band diagram of PVP (a) and PVP/ZnO nanocomposite (b) and the transitions related to the emission of light. The energies of all levels are counted from the vacuum level. Non-radiative transitions are not shown for simplicity

The incident visible light (exc. 2) causes another type of processes in the nanocomposite. Similarly to the case of pure polymer, in nanocomposites the energy of these quanta is also absorbed by defects in polymeric matrix (see arrow 2 in Fig. b). However, the excitation does not lead to emission by polymeric matrix. Instead, excitation is transferred to defect states in ZnO NPs and is deactivated by emitting ~ 480 nm light (arrows 3).

The observed transfer of excitation between the matrix and NPs correlates with the behavior of other organic/inorganic nanocomposites. In the case of ZnS:Ni nanoparticles that were redispersed into PVP [30] the emission band of was excited by the light with the wavelengths coinsiding with the matrix emission band. Moreover, the excitation within the matrix emission band was also demonstrated for Mn^{2+} impurities in ZnS:Mn/PVP nanocomposite PVP [20]. Therefore, one can conclude that the excitation of the defects in NPs via polymeric matrix is a common feature of the emission of NPs embedded in PVP.

Different transfer mechanisms can be discussed as possible origins of the excitation of nanoparticles via the polymer matrix. They are: the reabsorption of the polymeric blue emission by NPs; non-radiative energy transfer from the matrix to NPs according to dipole-dipole interaction mechanism. In coordination bond formation between the nitrogen atom of PVP and Zn^{2+} was suggested as one of the important reasons giving rise to excitation transfer [16, 20]. This bond causes overlapping of molecular orbitals of PVP with atomic orbitals of metal ions in surface regions. It was

suggested that it can cause transfer of electron from the passivating layers of PVP around the nanoparticles to their luminescence centers [30]. However, at present additional studies are necessary to discriminate between different energy transfer mechanisms.

5. CONCLUSION

We have successfully synthesized ZnO/PVP colloids. The synthesis was carried out at low temperature, and the reaction conditions are environmentally friendly. Therefore this way of synthesis has many advantages as compared with other vapor deposition and physical processes. Solid composites films were obtained.

Bases on the results of photoluminescence and photolumenescence excitation studies of nanocomposites the energy levels diagram of nanocomposite was proposed, as well as the scheme of emission-related transitions. It was suggested that: (i) the high energy band in the PLE spectrum of nanocomposites arises from the PVP molecules within the polymeric constituent of nanocomposite while low energy PL band arises from ZnO nanoparticles; (ii) excitation of light-emitting states in ZnO nanoparticles occurs via energy transfer from the energy levels of PVP molecular orbitals.

REFERENCES

1. A.B. Djurisic, A.M.C. Ng, X.Y. *Chen, Prog. Quant. Electron.* **34**, 191 (2010).
2. Z.-Y. Zhang, H.-M. Xiong, *Materials* **8**, 3101 (2015).
3. F. Mikarajuddin, Iskandar, K. Okuyama, F.G. Shi, *J. Appl. Phys.* **89**, 6431 (2001).
4. L. Spanhel, M.A. Anderson, *J. Am. Chem. Soc.* **113**, 2826 (1991).
5. D. Jezequel, J. Guenot, N. Jouini, N.F. Fievet, *J. Mater. Res.* **10**, 77 (1995).
6. T. Vossmeyer, L. Katsikas, M. Giersig, I.G. Popovic, K. Diesner, A. Chemseddine, A. Eychmueller, H. Weller, *J. Phys. Chem.* **98**, 7665 (1994).

7. R. Viswanatha, S. Sapra, B. Satpati, P.V. Satyam, B.N. Dev, D.D. Sharma, *J. Mater. Chem.* **14**, 661 (2004).
8. V.A.L. Roy, A.B. Djurisic, W.K. Chan, J. Cao, H.F. Luiand, C. Surya, *Appl. Phys. Lett.* **83**, 141 (2003).
9. D.S. Bohleand, C.J. Spina, *J. Am. Chem. Soc.* **129**, 12380 (2007).
10. Y.H. Leung, A.B. Djurisic, Z.T. Liu, D. Li, M.H. Xieand, W.K. Chen, *J. Phys. Chem. Solids* **69**, 353 (2008).
11. A.C. Dodd, A.J. McKinley, M. Saundersand, T. Tsuzuki, *J. Nanopart. Res.* **8**, 43 (2006).
12. C.X. Shan, Z. Liuand, S.K. Hark, *Appl. Phys. Lett.* **92**, 073103 (2008).
13. Q-H. Chen, W-G. Zhang, *J. Non-Cryst. Solids* **353**, 374 (2007).
14. M.L. Kahn, T. Cardinal, B. Bousquet, M. Monge, V. Juberaand, B. Chaudret, *Chem. Phys. Chem.* **7**, 2392 (2006).
15. A.Y. Polyakov, N.B. Smirnov, A.V. Govorkov, E.A. Kozhukhova, S.J. Pearton, D.P. Norton, A. Osinsky, A. Dabiran, *J. Elec. Mater.* **35**, 663 (2006).
16. T.T. Minh, B.P. Van, T.D. Van, H.N. Thi, *Opt. Quan. Electron.* **45**,147 (2013).
17. I.H. Tang, R. Sundari, H.O. Lintang, L. Yuliati Malaysian, *J. Anal. Sci.* **20**, 288 (2016).
18. M. Behera, S. Ram, *Appl. Nanosci.* **3**, 543 (2013).
19. S. Ram, H.-J. Fecht, *J. Phys. Chem. C* **115**, 7817 (2011).
20. K. Manzoor, S.R. Vadera, N. Kumar, T.R.N. Kutty, *Solid State Commun.* **129**, No 7, 469 (2004).
21. H.-M. Xiong, *J. Mater. Chem.* **20**, 4251 (2010).
22. Q.P. Wang, X.J. Zhang, G.Q. Wang, S.H. Chen, X.H. Wu, H.L. Ma, *Appl. Surf. Sci.* **254**, 5100 (2008).
23. S. Chakrabarti, D. Ganguli, S. Chaudhuri, *J. Phys. D.* **36**, 146 (2003).
24. L.L. Yang, Q.X. Zhao, M. Willander, J.H. Yang, I. Ivanov, *J. Appl. Phys.* **105**, 053503 (2009).
25. L. Dong, Y.C. Liu, Y.H. Tong, Z.Y. Xiao, J.Y. Zhang, Y.M. Lu, D.Z. Shen, X.W. Fan, *J. Colloid Interf. Sci.* **283**, 380 (2005).
26. R. Xie, T. Sekiguchi, T. Ishigaki, N. Ohashi, D. Li, D. Yang, B. Liu, Y. Bando, *Appl. Phys. Lett.* **88**, 134103 (2006).
27. B. Cao, W. Cai, H. Zeng, *Appl. Phys. Lett.* **88**, 161101 (2006).
28. B. Lin, Z. Fu, Y. Jia, *Appl. Phy. Lett.* **79**, 943 (2001).
29. F. Meng, S. Liu, Y. Wang, C. Tao, P. Xu, W. Guo, L. Shen, X. Zhang, S. Ruan, *J. Mater. Chem.* **22**, 22382 (2012).
30. T.M. Thi, L.V. Tinh, B.H. Van, P.V. Ben, V.Q. Trung, *J. Nanomater. ID* **528047** (2012).